Reorganization of the microtubule array in prophase/prometaphase requires cytoplasmic dynein-dependent microtubule transport

Nasser M. Rusan, U. Serdar Tulu, Carey Fagerstrom, and Patricia Wadsworth

Department of Biology and Program in Molecular and Cellular Biology, Morrill Science Center, University of Massachusetts, Amherst, MA 01003

When mammalian somatic cells enter mitosis, a fundamental reorganization of the Mt cytoskeleton occurs that is characterized by the loss of the extensive interphase Mt array and the formation of a bipolar mitotic spindle. Microtubules in cells stably expressing GFP–α-tubulin were directly observed from prophase to just after nuclear envelope breakdown (NEBD) in early prometaphase. Our results demonstrate a transient stimulation of individual Mt dynamic turnover and the formation and inward motion of microtubule bundles in these cells. Motion of microtubule bundles was inhibited after antibody-mediated inhibition of cytoplasmic dynein/dynactin, but was not inhibited after inhibition of the kinesin-related motor Eg5 or myosin II. In metaphase cells, assembly of small foci of Mts was detected at sites distant from the spindle; these Mts were also moved inward. We propose that cytoplasmic dynein-dependent inward motion of Mts functions to remove Mts from the cytoplasm at prophase and from the peripheral cytoplasm through metaphase. The data demonstrate that dynamic astral Mts search the cytoplasm for other Mts, as well as chromosomes, in mitotic cells.

Introduction

During each cell cycle, a major reorganization of cellular components occurs in preparation for cell division. One particularly dramatic change is the loss of the extensive interphase Mt array and the subsequent assembly of a bipolar mitotic spindle. Spindle assembly has been extensively studied in both intact cells and cell extracts. The results of these experiments have clearly demonstrated that spindle assembly requires both dynamic Mts and various molecular motors that contribute to centrosome separation, spindle pole formation, and chromosome motion (for reviews see Inoué and Salmon, 1995; Sharp et al., 2000; Karsenti and Vernos, 2001). However, the mechanism by which the interphase Mt array is dismantled at the entry into mitosis is not as well understood. Previous analysis of PtK₁ cells has shown that loss of the interphase array is abrupt, beginning at, or just after, nuclear envelope breakdown (NEBD)* (Zhai et al.,

1996). Further measurements document a dramatic decrease in Mt polymer level and increase in the dynamic turnover of the population of Mts at NEBD (Zhai et al., 1996). However, to date, direct observations of individual Mts at the interphase to mitosis transition have not been reported.

To determine how the interphase Mt array is remodeled at the G2-M transition we have used spinning disc confocal microscopy (Waterman-Storer et al., 2000) to make real-time observations of Mt behavior in cells expressing GFP–α-tubulin (LLCPK1α; Rusan et al., 2001). Cells were examined from prophase to early prometaphase, just after NEBD. We demonstrate that at NEBD Mt dynamic instability behavior is transiently stimulated, and that bundles of Mts form and are transported toward the nuclear envelope (NE)/centrosome region in a cytoplasmic dynein-dependent manner.

Results and discussion

Early prophase cells are characterized by an intact nucleus, containing condensing chromosomes, and a Mt array that is indistinguishable from that in neighboring interphase cells (Fig 1). As prophase progresses, the NE becomes perforated (Fig. 1 A; Terasaki et al., 2001), and several minutes later begins to break down, releasing the condensed chromosomes (Beaudouin et al., 2002; Salina et al., 2002). We imaged the
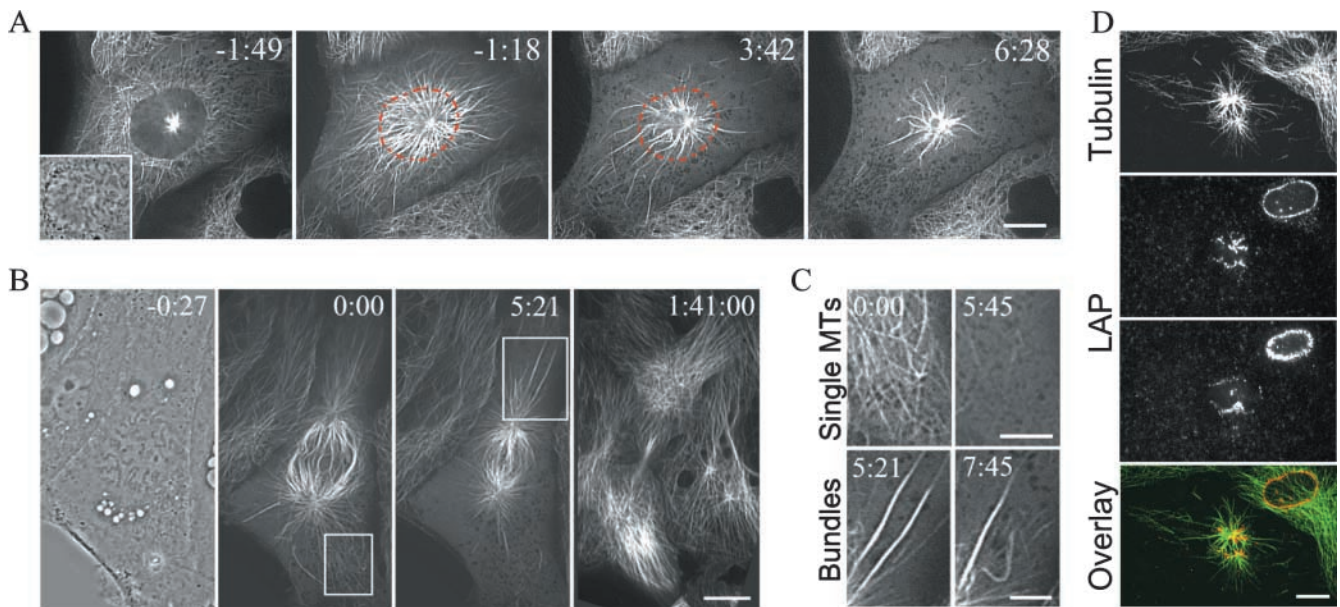
Figure 1. **Mt remodeling in prophase/metaphase cells.** (A) GFP-tubulin fluorescence in a prophase cell; time is relative to the onset of inward collapse of the Mt array. Inset in the first panel shows the nucleus in phase contrast; the focal plane was changed for subsequent panels. (B) Prophase cells imaged starting at NE perforation complete mitosis and cytokinesis normally; time as in A. (C) Higher magnification of the boxed regions in B show the rapid loss of individual Mts (top, single Mts) and the formation and motion of Mt bundles (bottom, bundles). (D) Immunofluorescence staining for Mts (top) and the inner NE protein LAP2 (middle, two different focal planes) and overlay (bottom). Inward collapse of the Mt array occurs at NEBD. Bars: (A, B and D) 10 μm; (C) 5 μm.

Mt array in cultured epithelial cells from NE perforation in prophase through NEBD and early prometaphase (Fig. 1 A). We observed both the rapid disassembly of individual Mts and the formation and motion of Mt bundles and foci (Fig. 1 C). The inward motion of the bundles resulted in a dramatic inward collapse of the Mt array (Fig 1 D) that coincided temporally with the initation of NEBD (Fig. 1 D). For this reason, we refer to these cells as prophase/prometaphase or at NEBD in this report. Cells observed as described completed mitosis and cytokinesis normally (Fig. 1 B). These features are clearly seen in Videos 1

and 2 (available at http://www.jcb.org/cgi/content/full/jcb.200204109/DC1).

To determine the mechanism responsible for the rapid loss of individual Mts at NEBD (Fig. 1 C), we quantified dynamic instability behavior of individual Mts (Mitchison and Kirschner, 1984); Mts with two free ends (Keating et al., 1997; Rusan et al., 2001) and Mts that contributed to bundle formation were not included in the quantitative analysis. The results demonstrate that Mt depolymerization at NEBD results from an increase in the duration and distance of shortening events, a decrease in pause duration and

Table I. **Dynamic instability parameters at microtubule plus ends**

Dynamic parameters	Interphase	NEBD	Metaphase
	62 MTs	30 MTs	28 MTs
Growth			
Rate (μm/min)	11.5 ± 7.40	10.7 ± 9.17	12.8 ± 5.66
Distance (μm)	1.22 ± 0.93	1.48 ± 1.44	3.14 ± 1.59[a]
Duration (s)	7.20 ± 4.96[a]	11.9 ± 11.1	17.0 ± 12.5
Shrink			
Rate (μm/min)	13.1 ± 8.43	12.3 ± 5.23	14.1 ± 7.86
Distance (μm)	1.52 ± 1.77[a]	4.00 ± 3.38	3.70 ± 3.83
Duration (s)	6.71 ± 4.28[a]	19.3 ± 14.0	13.2 ± 7.65[b]
Average pause duration	25.5 ± 32.7[c]	13.1 ± 14.5	9.31 ± 5.08
Percentage of time per phase (growth/shrink/pause)	15.0/11.5[a]/73.5[a]	16.1/49.6/34.3	50.5[a]/38.1/11.4[a]
Rescue frequency (s^{-1})	0.175 ± 0.104[a]	0.023 ± 0.029	0.045 ± 0.111
Catastrophe frequency (s^{-1})	0.026 ± 0.024[a]	0.075 ± 0.089	0.058 ± 0.045
Dynamicity (μm/min)	4.0 ± 3.5[a]	9.04 ± 3.95	14.6 ± 11.3

Dynamicity was determined by dividing the sum of the total length that the microtubule grew and shortened by the life span of the microtubule.
[a]Significant from NEBD cells at 99.9% confidence level.
[b]Significant from NEBD cells at 95% confidence level.
[c]Significant from NEBD cells at 99% confidence level.
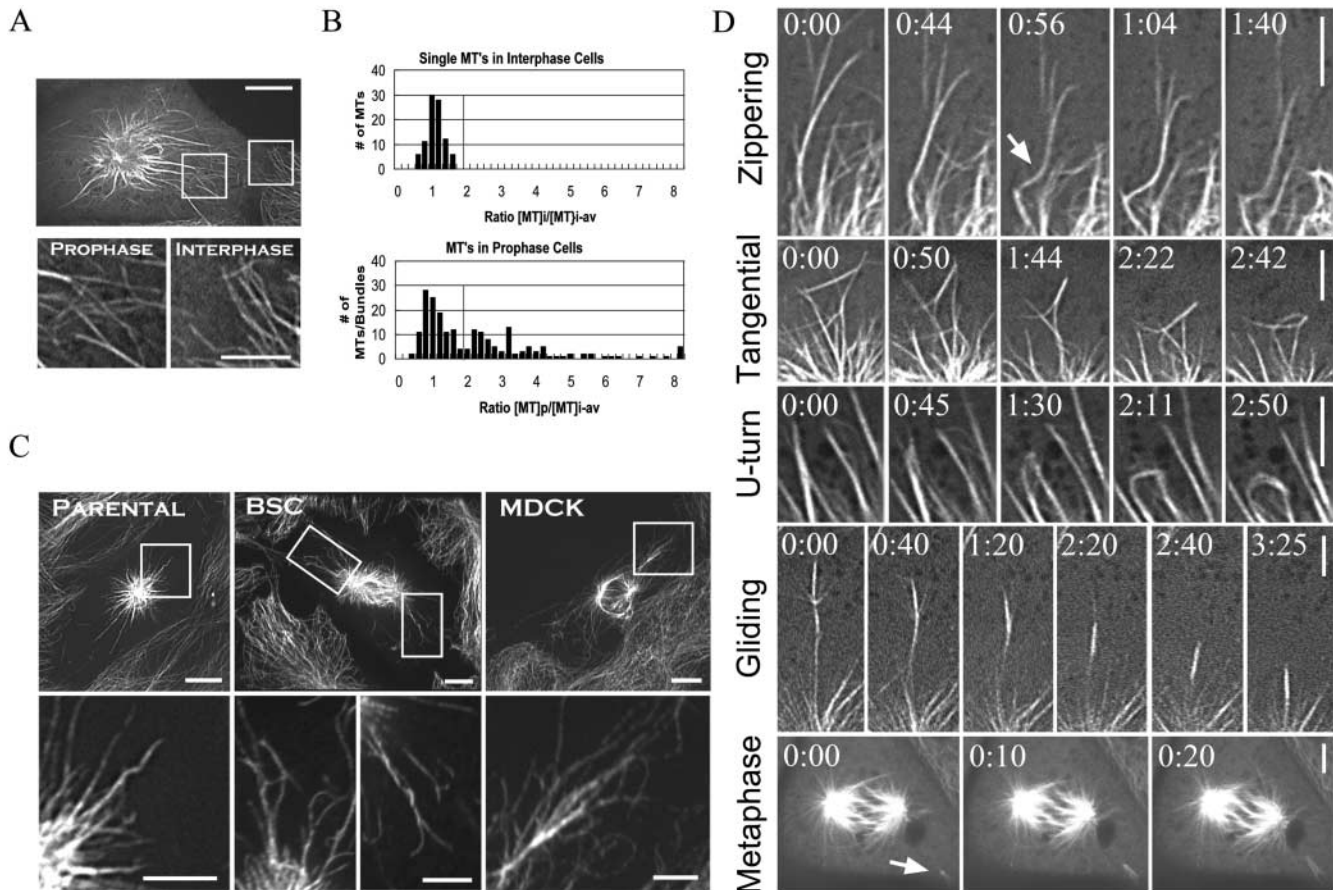All statistics were analyzed using a Student's t test.

Figure 2.   **Formation and motion of Mt bundles in prophase/prometaphase cells.** (A and B) Quantification of fluorescence intensity; boxed areas in A are enlarged below; (B) Histograms of normalized fluorescence intensity values. (C) Prophase Mt bundles, visualized using immunofluorescence, in LLCPK1 parental, BSC-1, and MDCK cells; boxed areas are enlarged below. (D) Motile behavior of Mts in prophase cells; times are the interval between successive images in min:s. Top four rows of panels are oriented so that the NE is to the bottom of each series; bottom row is a metaphase cell; arrow shows a small focus of Mts; the dark sphere is a vacuole. Bars: (A and C, top) 10 μm; (A and C, bottom, and D) 5 μm.

a decrease in the frequency of rescue events (Table I). Cell cycle–dependent changes in transition frequencies were greater between interphase and prophase than between interphase and metaphase; dynamicity was intermediate between interphase and metaphase values (Table I; Rusan et al., 2001). Thus, individual Mt dynamic instability behavior is transiently stimulated at NEBD in mammalian somatic cells (Tournebize et al., 2000).

Perhaps the most striking feature of the Mt cytoskeleton in prophase cells was the formation of Mt bundles and foci by the lateral association and clustering of Mts (Fig. 2). The Mt bundles are not an artifact of expression of GFP–α-tubulin because they were observed in the parental cell line, LLCPK1, and other epithelial cells, after fixation and staining with antibodies to tubulin (Fig. 2 C). To demonstrate that a bundle does in fact consist of more than one Mt, we measured the fluorescence intensity of GFP-tubulin containing bundles and individual Mts in prophase and neighboring interphase cells, respectively (Fig. 2 A). In interphase cells, fluorescence intensity values in a single pixel width (0.133 um) along a GFP-tubulin–containing Mt were tightly distributed around a single value (normalized to 1), whereas in cells at NEBD, values >1 were also observed

(Fig. 2 B). We did not measure the fluorescence intensity across the entire width of a bundle, so the measurement does not indicate the total number of Mts in a bundle.

Mt bundles at NEBD are highly dynamic and their motion was directed inward, toward the NE and associated centrosomes, not toward the periphery. Lateral zippering together of adjacent Mts is commonly observed; the resulting bundles buckle, and sometimes break, as they are moved inward (Fig. 2 D, zippering, arrow; Video 3 [available at http://www.jcb.org/cgi/content/full/jcb.200204109/DC1]). We also observed that Mts extend out from the central region of the cell and interact with noncentrosomal Mts lying parallel to the cell cortex. These interactions resulted in the tangential motion of the peripheral Mts toward the nucleus along the extending Mt(s) (Fig. 2 D, tangential; Video 4 [available at http://www.jcb.org/cgi/content/full/jcb.200204109/DC1]). The behavior of bent and buckling Mts, and the tangential interactions, show that Mts are moved or transported inward; treadmilling (Rodionov and Borisy, 1997) cannot account for these motions.

In some cells, Mts form a focus, or mini-aster, that associates with an extending Mt(s) (Fig. 2 D, gliding; Video 6 [available at http://www.jcb.org/cgi/content/full/
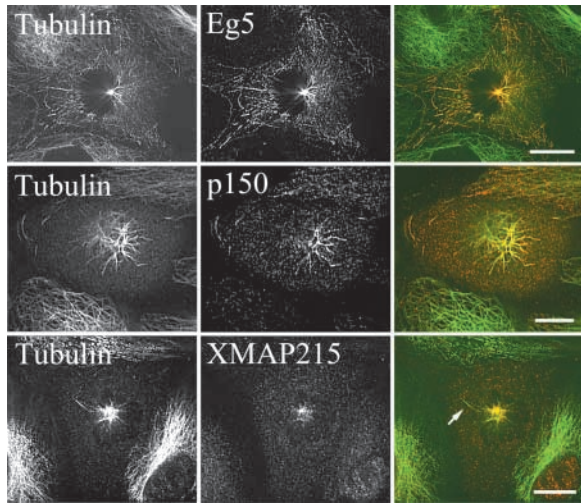
Figure 3. **Localization of Mt bundle components.** Immunolocalization of tubulin (left), Eg5 (top), dynactin (p150; middle), and XMAP215 (bottom) in fixed LLCPK1α cells; overlays (tubulin in green; Eg5, p150 and XMAP215 in red) are shown at right. Eg5 and p150, but not XMAP215, localize to the Mt bundles.

jcb.200204109/DC1]). The length of the extending Mt(s) decreases and the aster of Mts appears to move inward. Subunit loss from the Mt minus end could account for the motion and overall shortening of the Mt bundle. However, to
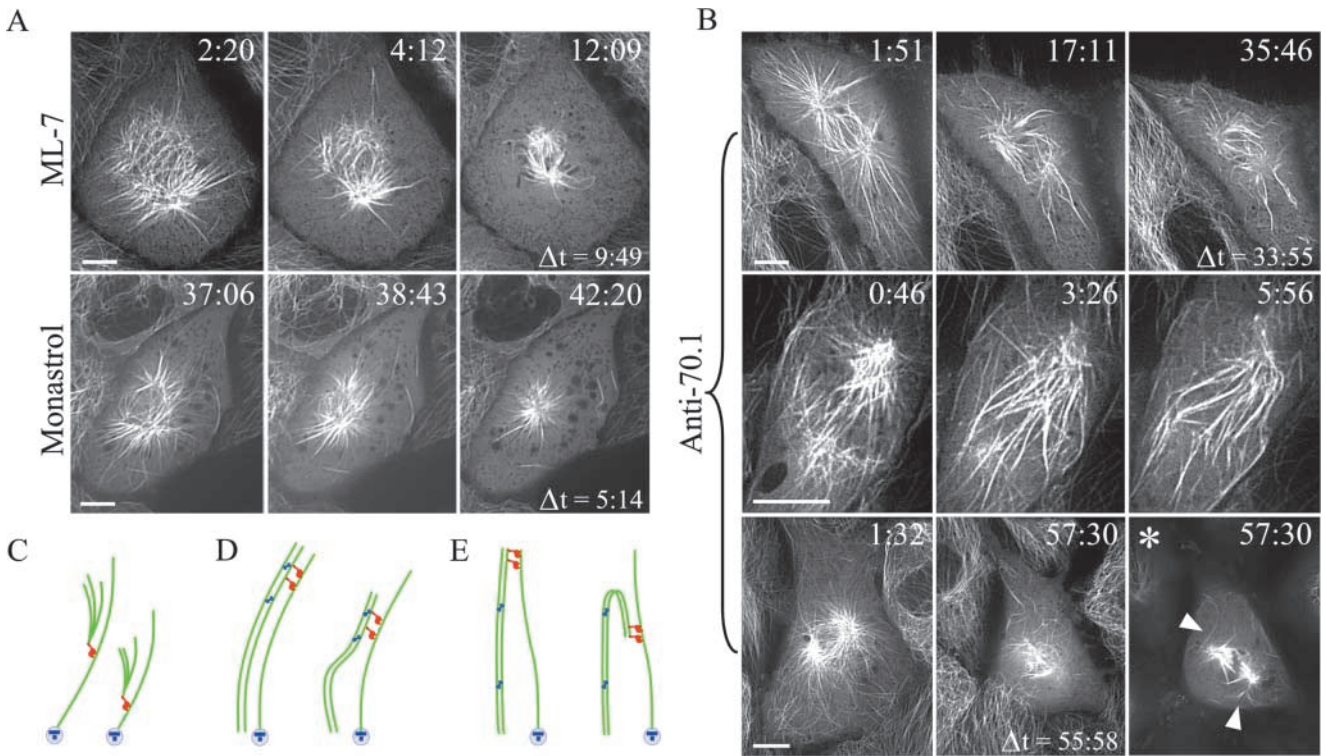
date, there is no evidence for loss of subunits from minus ends of astral Mts, thus we favor a mechanism involving sliding of the aster of Mts along an extending Mt and concomitant subunit loss from the plus-end.

The most unanticipated behavior we observed was the U-turn, in which the extending end of a bundle turned 180° and began moving toward the NE/centrosome. In this type of motion, the tip of the extending bundle appeared to interact with, and move inward along, an adjacent Mt bundle (Fig. 2, U-turn; Video 5 [available at http://www.jcb.org/cgi/content/full/jcb.200204109/DC1]).

The image sequences in Fig. 2 D, which are single confocal sections, also clearly demonstrate a dramatic decrease in Mt polymer level in prophase cells (Zhai et al., 1996). In addition to the disassembly of individual Mts (Fig. 1), Mt bundles decreased in length and fluorescence intensity, indicating that they undergo net disassembly as well. Preliminary observations indicate that the bundles continue to undergo dynamic rearrangements and are incorporated into the forming spindle (Video 2 [available at http://www.jcb.org/cgi/content/full/jcb.200204109/DC1]).

Immunolocalization was performed to determine the molecular composition of Mt bundles in prophase cells. The bipolar, plus end–directed kinesin related motor protein HsEg5, which contributes to centrosome separation in mitosis and aster assembly in mitotic extracts (Sawin et al., 1992; Mayer et al., 1999; Compton, 2000) was detected

Figure 4. **Dynein/dynactin-dependent motion of Mt bundles.** (A) Images of prophase LLCPK1α cells incubated with ML-7 (top) or monastrol (bottom). Time (min:s) after treatment is shown in the top right, elapsed time is shown in the bottom right. (B) Cells injected with anti-70.1 antibodies. Time after injection is shown in the top right. (Top) 33 min after injection bundles have formed, but inward motion is inhibited; elapsed time in the bottom right. (Middle) Inward collapse of bundles is inhibited in 70.1 injected cells. (Bottom) Spindle formation is abnormal in injected cells; asterisk indicates a different focal plane. (C–E) Models for Mt behavior at NEBD; cytoplasmic dynein moves clustered (C) and bundled (D and E) Mts toward the minus ends of centrosomal Mts. Bars, 10 μm.

along Mt bundles and in the centrosomal region of prophase cells (Fig. 3, top). Previous work has shown that the minus end–directed motor cytoplasmic dynein and its activator complex, dynactin, localize to the nuclear envelope in prophase cells (Salina et al., 2002) and on a subset of astral Mts from prophase through metaphase (Busson et al., 1998; O'Connell and Wang, 2000). Antibodies to the p150 (Fig. 3, middle) and ARP (not depicted) components of dynactin and to the intermediate chain of cytoplasmic dynein (not depicted) stained Mt bundles in prophase cells. Dynein and dynactin distributions were discontinuous along the length of the Mt and not all Mts were stained (Busson et al., 1998; O'Connell and Wang, 2000). Antibodies to XMAP215 stained spindle Mts in LLCPK1 cells (Fig. 3, bottom), but staining of astral Mts in mitotic cells, Mt bundles in prophase cells, and interphase Mts was not detected (Tournebize et al., 2000).

We tested the role of molecular motors in the motion of Mt bundles. Recent work has shown that Mts are moved in interphase cells by myosin II (Yvon and Wadsworth, 2000; Yvon et al., 2001), so we examined the effect of the myosin light chain kinase inhibitor, ML-7, on Mt behavior at entry into mitosis. In prophase cells treated with ML-7, no change in the formation or motile behavior of Mt bundles was detected (Fig 4 A). We also measured clearance time, defined as the interval from the initiation of Mt array collapse until a zone one third the diameter of the cell was free of both individual Mts and Mt bundles. Clearance time in ML-7–treated cells (6.1 ± 1.4 min, $n = 4$) was not different from control cells (7.8 ± 3.9 min; $n = 14$), indicating that myosin II activity does not contribute to Mt rearrangements in prophase cells (Fig. 4 A).

To determine if Eg5 contributes to Mt behavior at NEBD, we used monastrol, a specific inhibitor of Eg5 (Mayer et al., 1999). No changes in Mt bundle formation or motion were detected in cells treated with monastrol at prophase or up to 30 min prior to prophase. Clearance time (6.8 ± 2.8 min, $n = 4$) was not different from controls (7.8 ± 3.9 min, $n = 14$). Note that treatment with monastrol resulted in monopolar spindle formation demonstrating that the monastrol inhibited centrosome separation in these cells (Fig. 4 A).

To determine the role of cytoplasmic dynein in prophase Mt motion, antibodies to the cytoplasmic dynein intermediate chain, clone 70.1, that block cytoplasmic dynein function by inhibiting its association with the dynactin complex, were microinjected into prophase cells (Heald et al., 1997; Compton, 2000). In these cells, Mt bundles formed, but the inward collapse of the Mt array was inhibited (Fig. 4 B, top). Mt bundles in 70.1 injected cells appeared noticeably less rigid than in controls (Fig. 4 B, middle). Individual Mt disassembly was not inhibited in 70.1 injected cells (Fig. 4 B), resulting in some polymer loss and partial Mt clearance. However, clearance time could not be measured because bundles remained in each of the seven injected cells for the duration of the experiment (22–75 min). Note that some bundle motion, which lacked directionality, was detected, indicating that other motors may contribute to Mt rearrangements at NEBD (Mountain et al., 1999; Compton, 2000; Sharp et al., 2000). As expected, spindle formation

was abnormal in 70.1 injected cells (Fig. 4 b, bottom; Compton, 2000).

Although the rate of bundle motion could not be measured in 70.1 injected cells, the rate of bundle motion in control cells (5.5 ± 3.0 um/min; $n = 18$, 9 cells) was slower than the rate of dynein driven Mt motion in vitro, but remarkably similar to the rate of dynein dependent motion of Mt seeds along spindle Mts in *Xenopus* extracts (Heald et al., 1996).

During observation of many mitotic cells expressing GFP–α-tubulin, we occasionally observed the formation of small foci of Mts in mitotic cytoplasm at sites distant from the spindle. Once formed these Mts are cleared from the cytoplasm in a manner strikingly similar to the behavior of Mt bundles in prophase cells (Fig. 2 D, metaphase). Clearance occurs when an astral Mt extending from the centrosome (not visible in Fig. 2 D) interacts with the peripheral Mts. Because ectopic Mt foci arise infrequently, we were not able to directly test the mechanism of their motion. However, injection of clone 70.1 antibodies into metaphase cells induced a rapid outward expansion of the spindle (unpublished data), demonstrating that cytoplasmic dynein generates inward directed forces throughout metaphase (Compton, 2000) and thus could contribute to inward motion of Mt foci. Our data demonstrate that non-spindle Mts can assemble in the peripheral regions of mitotic cells and that when this occurs, they are rapidly cleared from the periphery and moved to the spindle region. A common feature of all these motions is the movement of one or more Mts along another (Fig. 4, C–E) demonstrating that Mts are the cargo of minus end–directed cytoplasmic dynein in mitotic cells (Heald et al., 1997).

The results of these experiments demonstrate that two mechanisms contribute to the remodeling of the Mt array at entry into mitosis: a change in the parameters of Mt dynamic instability and cytoplasmic dynein dependent inward motion of Mt bundles. Are both mechanisms required for Mt remodeling at the entry into mitosis? One possibility is that these mechanisms are functionally redundant and that either could accomplish clearance of the peripheral Mts in the absence of the other. The second possibility, the one we favor, is that both mechanisms are needed for Mt clearance at NEBD. The two different mechanisms may be used to remodel subsets of interphase Mts that differ in their dynamic behavior (Bre et al., 1990; Wadsworth and Bottaro, 1996). Dynamic interphase Mts may be rapidly disassembled by the global change in dynamic instability, whereas the more stable subset may form bundles that are subsequently moved by cytoplasmic dynein. This possibility is consistent with the observation that interphase LLCPK1 cells contain numerous stable Mts (Rusan et al., 2001). However, Mt bundles are dynamic, indicating that motion and disassembly function cooperatively, not just independently. The requirement for both mechanisms is also supported by the observation that when Mt dynamics were suppressed with low concentrations of taxol (unpublished data) collapse of the Mt array was observed, but individual Mts were not completely cleared. Similarly, when cytoplasmic dynein was inhibited, Mt disassembly continued but did not compensate for the lack of

bundle motion. Finally, we note that an advantage of the cytoplasmic dynein dependent pathway is that Mt polymer is delivered to the site of spindle formation, to which it could directly contribute (Video 2).

In conclusion, our data document a novel role for cytoplasmic dynein/dynactin in the inward directed motion of Mts at NEBD. Together with other recent results we propose that cytoplasmic dynein plays a key role at prophase/prometaphase by temporally coordinating NEBD (Beaudouin et al., 2002; Salina et al., 2002) and the inward collapse of the Mt array. The data support a model in which centrosomally nucleated Mts search the cytoplasm for other Mts and mediate their inward transport. Eliminating Mts from the periphery could prevent chromosome interactions with non-spindle Mts and thus increase mitotic fidelity.

Materials and methods

Materials
All materials for cell culture were obtained from Life Technologies/GIBCO-BRL, with the exception of fetal calf serum, which was obtained from Atlanta Biologicals. Unless otherwise noted, all other chemicals were obtained from Sigma-Aldrich.

Cell culture and cell growth assays
LLCPK1α cells were cultured in OptiMEM supplemented with 1 mM sodium pyruvate, 5% fetal calf serum, and antibiotics, in an atmosphere of 5% CO_2, at 37°C. MDCK cells were grown in DME; BSC1 cells were grown in MEM.

Immunofluorescence microscopy
The following antibodies were used in these experiments: anti-Arp1, a gift of Dr. T. Schroer (Johns Hopkins University, Baltimore, MD); anti-p150 and anti-LAP2 (Transduction Laboratories); anti-tubulin, clone DM1a, and anti-dynein, clone 70.1 (Sigma-Aldrich); anti-dynein clone 74.1 (Chemicon International, Inc.); anti-XMAP 215, a gift of Dr. A. Popov (European Molecular Biology Laboratory, Heidelberg, Germany); and anti-HsEg5, a gift of Dr. D. Compton (Dartmouth Medical School, Hanover, NH). Cells were fixed in methanol (p150, LAP2, Arp1, Eg5, 70.1, 74.1) (Yvon and Wadsworth, 2000) or with paraformaldehyde/glutaraldehyde (XMAP215) as described (Tournebize et al., 2000). Incubations with primary antibodies were performed overnight at room temperature or for 1 h at 37°C; Cy-3 (Jackson ImmunoResearch Laboratories) or FITC-labeled secondary antibodies (ICN Biomedicals, Inc.) were used at the recommended dilution for 1 h at room temperature. Coverslips were mounted in Vectashield (Vector laboratories) and sealed with nail polish.

Image acquisition
Images were acquired using a Nikon Eclipse TE 300 microscope equipped with a 100× phase, NA 1.4 objective lens, a Perkin Elmer Spinning Disc Confocal Scan head (Perkin Elmer) and a Roper Micromax interline transfer cooled CCD camera (Roper Scientific) All images were taken using a single wavelength (488) filter cube. Image acquisition was controlled by Metamorph Software (Universal Imaging Corp.). Time-lapse sequences were acquired at 2-s intervals using an exposure time of 0.3–0.7 s. Tracking Mts and statistical analysis were performed exactly as described (Rusan et al., 2001). Quantification of fluorescence intensity was performed by measuring the fluorescence intensity in a 10-pixel long segment of a Mt/Mt bundle and subtracting the average background fluorescence of the same sized region, measured on either side of the Mt/Mt bundle. Normalized values were plotted.

Inhibition experiments
For inhibition of cytoplasmic dynein, coverslips were mounted in a Rose chambers and injected with antibodies to the intermediate chain of dynein, prepared as described previously (Yvon et al., 2001). Each batch of concentrated antibody was tested by microinjection into interphase cells followed by fixation and staining for 58K Golgi protein; the lowest dilution of antibody that resulted in 100% of cells showing Golgi dispersion was used for experiments. Monastrol (Calbiochem) was used at 100 uM; ML-7 was used exactly as described (Yvon et al., 2001).

Online supplemental material
Movie sequences corresponding to the cell shown in Fig. 1 A (Video 1), a supplemental sequence of two prophase cells (Video 2), and sequences corresponding to the top four rows of panels in Fig. 2 D (Videos 3–6) are provided. A panel showing individual microtubule behavior (Fig. 1 E) is also provided.

References

Beaudouin, J., D. Gerlich, N. Daigle, R. Eils, and J. Ellenberg. 2002. Nuclear envelope breakdown proceeds by microtubule-induced tearing of the lamina. *Cell.* 108:83–96.

Bre, M.-H., R. Pepperkok, A.M. Hill, N. Levilliers, W. Ansorge, E.H.K. Stelzer, and E. Karsenti. 1990. Regulation of microtubule dynamics and nucleation during polarization in MDCK II cells. *J. Cell Biol.* 111:3013–3021.

Busson, S., D. Dujardin, A. Moreau, J. Dompierre, and J.R. DeMay. 1998. Dynein and dynactin are localized to astral microtubules and at cortical sites in mitotic epithelial cells. *Curr. Biol.* 8:541–544.

Compton, D.A. 2000. Spindle assembly in animal cells. *Annu. Rev. Biochem.* 69:95–114.

Heald, R., R. Tournebize, T. Blank, R. Sandaltzopoulos, P. Becker, A.A. Hyman, and E. Karsenti. 1996. Self-organization of microtubules into bipolar spindles around artificial chromosomes in *Xenopus* egg extracts. *Nature.* 382:420–425.

Heald, R., R. Tournebize, A. Habermann, E. Karsenti, and A. Hyman. 1997. Spindle assembly in *Xenopus* egg extracts: respective roles of centrosomes and microtubule self-organization. *J. Cell Biol.* 138:615–628.

Inoué, S., and E.D. Salmon. 1995. Force generation by microtubule assembly/disassembly in mitosis and related movements. *Mol. Biol. Cell.* 6:1619–1640.

Karsenti, E., and I. Vernos. 2001. The mitotic spindle: a self-made machine. *Science.* 294:543–547.

Keating, T.J., J.G. Peloquin, V.I. Rodionov, D. Momcilovic, and G.G. Borisy. 1997. Microtubule release from the centrosome. *Proc. Natl. Acad. Sci. USA.* 94:5078–5083.

Mayer, T.U., T.M. Kapoor, S.J. Haggarty, R.W. King, S.L. Schreiber, and T.J. Mitchison. 1999. Small molecule inhibitor of mitotic spindle bipolarity identified in a phenotype-based screen. *Science.* 286:971–974.

Mitchison, T.J., and M.W. Kirschner. 1984. Dynamic instability of microtubule growth. *Nature.* 312:237–242.

Mountain, V., C. Simerly, L. Howard, A. Ando, G. Schatten, and D.A. Compton. 1999. The kinesin-related protein, HSET, opposes the activity of Eg5 and cross-links microtubules in the mammalian mitotic spindle. *J. Cell Biol.* 147:351–365.

O'Connell, C.B., and Y.I. Wang. 2000. Mammalian spindle orientation and position respond to changes in cell shape in a dynein-dependent fashion. *Mol. Biol. Cell.* 11:1765–1774.

Rodionov, V.I., and G.G. Borisy. 1997. Microtubule treadmilling *in vivo. Science.* 275:215–218.

Rusan, N.M., C. Fagerstrom, A.C. Yvon, and P. Wadsworth. 2001. Cell cycle dependent changes in microtubule dynamics in living cells expressing GFP-alpha tubulin. *Mol. Biol. Cell.* 12:971–980.

Salina, D., K. Bodoor, D.M. Eckley, T.A. Schroer, J.B. Rattner, and B. Burke. 2002. Cytoplasmic dynein as a facilitator of nuclear envelope breakdown. *Cell.* 108:97–107.

Sawin, K.E., K. LeGuellec, M. Philippe, and T.J. Mitchison. 1992. Mitotic spindle organization by a plus-end directed microtubule motor. *Nature.* 359:540–543.

Sharp, D.J., G.C. Rogers, and J.M. Scholey. 2000. Microtubule motors in mitosis. *Nature.* 407:41–47.

Terasaki, M., P. Campagnola, M.M. Rolls, P.A. Stein, J. Ellenberg, B. Hinkle, and B. Slepchenko. 2001. A new model for nuclear envelope breakdown. *Mol. Biol. Cell.* 12:503–510.

Tournebize, R., A. Popov, K. Kinoshita, A.J. Ashford, S. Rybina, A. Pozniakovsky, T.U. Mayer, C.E. Walzak, E. Karsenti, and A.A. Hyman. 2000. Control of

microtubule dynamics by the antagonistic activities of XMAP215 and XKCM1 in *Xenopus* egg extracts. *Nat. Cell Biol.* 2:13–19.

Wadsworth, P., and D. Bottaro. 1996. Microtubule dynamic turnover is suppressed during polarization and stimulated in HGF scattered MDCK epithelial cells. *Cell Motil. Cytoskeleton.* 35:225–236.

Waterman-Storer, C., D.Y. Duey, K.L. Weber, J. Keech, R.E. Cheney, E.D. Salmon, and W.M. Bement. 2000. Microtubules remodel actomyosin networks in *Xenopus* egg extracts via two mechanisms of F-actin transport. *J. Cell Biol.* 150:361–376.

Yvon, A.C., and P. Wadsworth. 2000. Region specific microtubule transport in motile cells. *J. Cell Biol.* 151:1003–1012.

Yvon, A.C., D.J. Gross, and P. Wadsworth. 2001. Antagonistic forces generated by myosin II and cytoplasmic dynein regulate microtubule turnover, movement, and organization in interphase cells. *Proc. Natl. Acad. Sci. USA.* 15: 8656–8661.

Zhai, Y., R.J. Kronebusch, P.M. Simon, and G.G. Borisy. 1996. Microtubule dynamics at the G2/M transition: abrupt breakdown of cytoplasmic microtubules at nuclear envelope breakdown and implications for spindle morphogenesis. *J. Cell Biol.* 135:201–214.